SILESIAN UNIVERSITY OF TECHNOLOGY

FACULTY OF CHEMISTRY

DEPARTMENT OF ORGANIC CHEMISTRY, BIOORGANIC CHEMISTRY AND BIOTECHNOLOGY

GRZEGORZ STANDO, MSc

Extended abstract of doctoral dissertation

Development of high-performance composites based on non-functionalized carbon nanostructures

Supervisor: Dawid Janas, Ph.D. DSc

GLIWICE 2023

Aims, scope, and hypothesis

This scientific work aimed to verify the hypothesis "pure nanocarbon surface is wettable with water and aromatic hydrocarbons are the reason for their apparent hydrophobicity." The doctoral dissertation results from initial research, which started in 2017. The results of these studies were as follows: thermally annealed carbon nanotubes exhibit surprisingly high wettability with water[1] and exhibit adsorption of compounds, which might cause the hydrophobicity of these materials[2]. In addition, earlier literature studies conducted by scientific groups of Prof. Lei Li and Prof. Haitao Liu from the University of Pittsburgh in the United States discovered that graphene and graphite are also strongly hydrophilic upon purification. However, to this date, the group of compounds responsible for the phenomenon remains unknown in the literature (especially for 0D and 1D nanocarbon). What is more, the mechanism of hydrophobization of nanocarbon surface has not been proposed. Other research groups observed the analogous impact of impurities on wettability of 2D materials such as hexagonal MoS_2 and BN, supporting the central hypothesis of the thesis [3]. To understand the mentioned phenomenon, three carbon nanomaterials and one material have been chosen: 0D – fullerene C_{60}, 1D – single-walled carbon nanotubes (SWCNTs), 2D – single layer graphene (SLG), and 3D – highly oriented pyrolytic graphite (to analyze the impact of number of graphene layers) (HOPG). Both experimental results and theoretical models were engaged to fill this research gap.

The second hypothesis of the dissertation is the implication of the first one: "Functionalization of carbon nanostructure is not always needed to manufacture high-performance composites with other materials since they can be made hydrophilic by thermal annealing without change to the structure or composition of the material." Without hydrophilic functional groups on the nanocarbon surface, composites should have much better properties, and it would improve the application potential of the material as thermoelectric generators, supercapacitors, or membranes.

Part of the dissertation is already published[3–6]. One more article is currently under preparation for submission to peer-review evaluation.

Description of the subject of research

Nanocarbon materials were discovered and described at the end of the XX century [7]. However, they are still intensively researched due to their properties: mechanical[8], chemical[9], electrical[10], optical[11], and thermal[12]. On the other hand, macroscopic objects from pure nanocarbon materials do not have such good properties[13], so they are used in connection with other materials like polymers and metals[14–16]. One of the most popular ways of increasing affinity between nanocarbon structures and other materials is functionalization – the insertion of hydrophilic groups into the nanostructure surface[17]. During this process, the pristine nanostructure is damaged, and it causes the changing of the properties of nanocarbon material[1,18–22]. As mentioned earlier, carbon nanostructures are considered hydrophobic, despite evidence that their true nature is the opposite. Thus understanding true surface character might improve the properties of composites from nanocarbon structures. The presence of functional groups might be unnecessary to improve integration between the compounds of composite. What is more, the composites based on hydrophilic non-functionalized nanocarbon structure should have better properties due to the lack of imperfections caused by chemical functionalization.

The general methodology employed to create macroscopic ensembles from nanocarbon materials

Synthesis of C_{60} is a multi-step reaction with a yield between 50-70%[23]. Thus, it was decided to use commercial material due to the high quality of such material and relatively low-cost compared to the costs of synthesis. The same situation was for single walled-carbon nanotubes.

The methods of manufacturing macroscopic objects from nanocarbon were as follows:

a) 0D – C_{60}: spray-coating;
b) 1D – single-walled carbon nanotubes (SWCNTs);
   - filtration method to create VFF *(vacuum filtration film)*;
   - dispersion method to obtain DF (*dispersion film)*;
c) 2D – single-layer graphene (SLG): in situ synthesis on copper by chemical vapor deposition (CVD).

Using VFF allows understanding of the interaction between nanocarbon and airborne contaminants/polymers. However, VFF was unsuitable for application in electrochemical synthesis composites with polyaniline (PANI) and copper due to too small dimensions. Thus the DF was cut to small electrodes (DFEs) and used exclusively in electrochemical experiments. On the other hand, VFF was used to investigate the phenomenon of hydrophobization, deposition of vaporized hydrocarbons, and synthesis of composites with poly(methyl methacrylate).

Main results

The results of the dissertation proved the proposed hypothesis that the true surface of nanocarbon materials is hydrophilic and proposed the mechanism of the phenomenon of hydrophobization nanocarbon surface. Chapter 4.1 *Hydrophobic or Hydrophilic? – understanding the wettability of nanocarbon materials and the phenomenon of their hydrophobization in the air* described the investigation of the phenomenon. Firstly it was researched the contact angle before and after annealing of surface macroscopic objects from C_{60} (0D material), SWCNTs (1D material), and SLG (2D material) (Figure 1). Annealing caused the hydrophilization nanocarbon surface – WCA for C_{60} before annealing was 138.3±0.8º and after 0.0±0.0º, SWCNTs before was 81.3±3.5º (top side) and after 0.0±0.0º, SLG on copper base before 82.9±1.5º and after 41.8±2.1º. Additionally, it was investigated the surface of HOPG (3D material) to understand the effect of the base on the graphene surface. Exfoliation was used to eliminate the surface contamination and reduced WCA from 96.9±2.9º → 63.8±2.1º. The results of spectroscopy analysis did not manifest any insertion of functional groups during the annealing process, which could cause the hydrophilization (Figure 2 presents the results of XPS analysis samples before and after annealing). Then the samples were exposed to two kinds of hydrocarbon: benzene (aromatic compound, sp^2 carbon) and cyclohexane (cycloalkane, sp^3 carbon) (Figure 3). It was demonstrated that aromatic structures caused the stronger hydrophobization of nanocarbon surfaces than saturated hydrocarbons. Thus it was assumed that they are a reason for the hydrophobic nanocarbon surface. The next step was to investigate the phenomenon of hydrophobicity nanocarbon surface by deposition of selected vapor aromatic hydrocarbons onto its and monitoring the evolution of surface character by WCA in of exposition to air (Figure 4). The collected data was analyzed by the Fowkes model, and it was observed that the deposit of hydrocarbon contamination decreased the polarity of the nanocarbon surface, which caused the hydrophobization of nanocarbon materials (Figure 5).

The XPS (Figure 6) and FTIR spectra allow us to propose the mechanism of the phenomenon: the first step is the adsorption of water from the environment, which is replaced by hydrocarbons. The presence of adsorbed aromatic hydrocarbons is the reason for the hydrophobicity of nanocarbon structures.

As was mentioned, only the SWCNTs macroscopic was free-standing, and it was the reason why they are used to create composites and understand the impact of functional groups on the properties of nanocomposite (lack of base effect). SWCNTs were oxidized by a modified Hummers method to use them as reference material for composites. It was researched the effect of process parameters on electrical conductivity and wettability of final product – O-SWCNTs. I_D/I_G ratio was used to monitor the process of oxidation. Increasing the temperature, time, or amount of $KMnO_4$ (oxidation agent) caused the growth I_D/I_G in chosen range (Figure 7 and 8). As it was expected, increasing the number of functional groups (growth of I_D/I_G) resulted in more hydrophilic surfaces of O-SWCNTs VFF but decreased their electrical conductivity of them (Figure 9).

Next, the phenomenon of hydrophilization of nanocarbon surfaces was applied to manufacture high-performance composites based on nanocarbon materials. Three types of composites were made by connecting nanocarbon materials with poly(methyl methacrylate) (PMMA), different kinds of polyaniline (PANI), and copper:

a) In the case of PMMA, the VFFs from SWCNTs and O-SWCNTs were applied to understand the impact of adsorbed hydrocarbons on the nanocarbon surface and functionalization on manufacturing the composites. Removing of surface contaminates caused radical growth of mass PMMA deposition onto carbon surface – 3.36 times compared to before annealing SWCNTs VFF. The presence of functional oxygen groups decreased the growth of mass PMMA deposits (Figure 10). What is more, O-SWCNTs and their composites have worse mechanical properties compared to SWCNTs and PMMA+SWCNTs (Figure 11).
b) DFE from SWCNTs and O-SWCNTs were used to manufacture the composites of nanocarbon with PANI by electropolymerization. To manufacture composites with PANI, three oxidation state of PANI was synthesized onto the nanocarbon surface: pernigraline, leucoemeraldine, and emeraldine (base and salt) by electropolymerization (EP). It was observed that the hydrophilicity of composites composed with emeraldine salt (ES) and SWCNTs (ES+SWCNTs) decreases with the growth number of EP cycles (Figure 12). The effect of functional groups was

negative for EP and electrical properties of nanocomposites. The increase in the number of functional groups on SWCNTs caused a decrease in the mass of PANI synthesized on their surface, as well as a decrease in the electrical conductivity of composites composed with O-SWCNT and PANI (Figure 13). The oxidative state of PANI was defined by: Raman spectroscopy, XPS, and electrical resistance measurements (Figure 14). Furthermore, it was observed the effect of doping SWCNTs by emeraldine salt, which responded to electrical conductivity improvement. The rest of the PANI forms caused decreasing in electrical conductivity composites compared with SWCNTs electrode. The electrical and thermoelectrical properties were measured to establish the potential of synthesized material as a supercapacitor and thermogenerator. The supercapacitor from ES+SWCNTs, after 5 cycles of EP, has the highest capacity (Figure 15). The ES+SWCNTs has the best thermoelectrical properties, but the enhancement was not high compared to pristine SWCNTs (Figure 16).

c) Hydrophilic DFE after annealing nanocarbon was used to recover copper from industrial wastewater and create composites of copper and nanocarbon. Firstly, it was used synthetic solution of copper to select the most promising material for Cu recovery. After that, selected materials were used for copper deposition from wastewater, where the Cu concentration was 428 ppm. The results of SEM (Figure 17) and EDX (Figure 18) analysis proved that Copper was deposited selectively onto the nanocarbon surface and creates a copper-nanocarbon nanocomposites, despite the fact number presence of other metals in higher concentrations like Fe, Al, or Mg (Table 1).

Conclusions

The dissertation hypothesis' were proved by performance studies. Under specific conditions, i.e., in the absence of hydrocarbons, carbon nanostructures exhibit a strongly hydrophilic character. The mechanism of this phenomenon seems to be as follows: polar nanocarbon surface adsorbs water from the air, which is then gradually replaced by methyl-benzene derivatives. As a result, the WCA value of these materials highly depends on air composition and will evolve in time due to environmental factors. The π-π stacking interactions stabilize the connection between nanocarbon material and hydrocarbon, impeding integration with other materials like metals or polymers. The results of the thesis show that by removing the surface impurities, the connection between nanocarbon and hydrophilic materials may be enhanced. Therefore, the most popular method for hydrophilization of nanocarbon material – destructive chemical functionalization appears not necessary for all of the cases. Such processing causing the insertion of hydrophilic groups creates many defects in carbon nanostructures, which reduces its properties, for example, electrical conductivity. The composites manufactured from highly-functionalized carbon nanostructures have much worse electrical and mechanical properties than composites based on annealed non-functionalized nanocarbon materials. This strategy allowed the creation of high-performance composites with polymers and metals. Furthermore, DFEs made from SWCNTs after annealing selectively recovered copper from industrial wastewater, wherein copper concentration was negligible in contrast to other metal ions.

To sum up, surface impurities have a significant impact on the surface character of carbon nanomaterials and thus on the properties of composites made of them according to presented results. The developed strategy for the manufacture of composites from non-functionalized carbon nanostructures can be used in the development of new techniques for the production of nanocarbon composites with better physicochemical properties than those used so far.

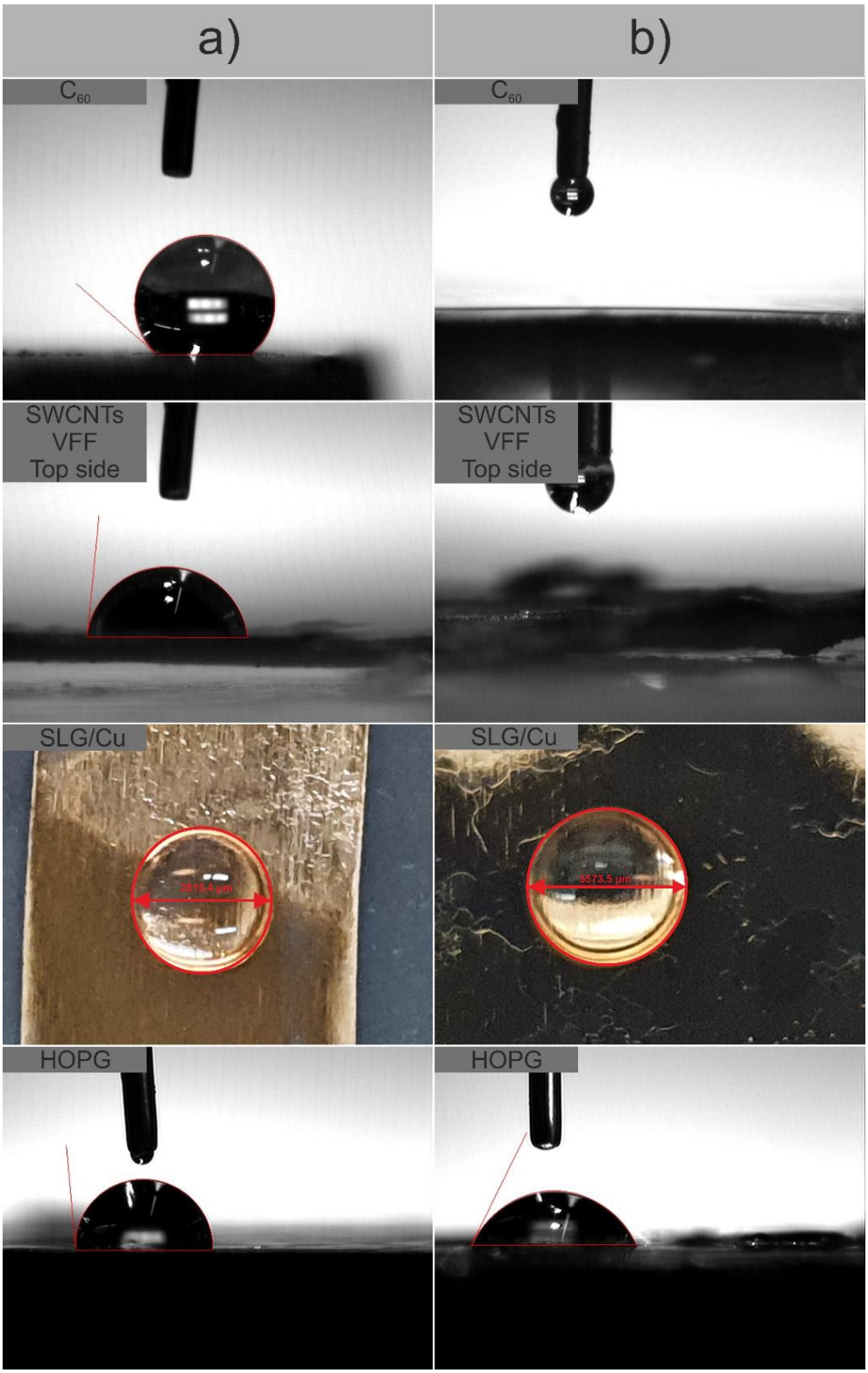

Figure 1. WCA measurements before (a) and after (b) the surface purification process: C_{60} and SLG/Cu were annealed in an atmosphere mixture of hydrogen and argon, SWCNT VFF were annealed in air, and HOPG was exfoliated.

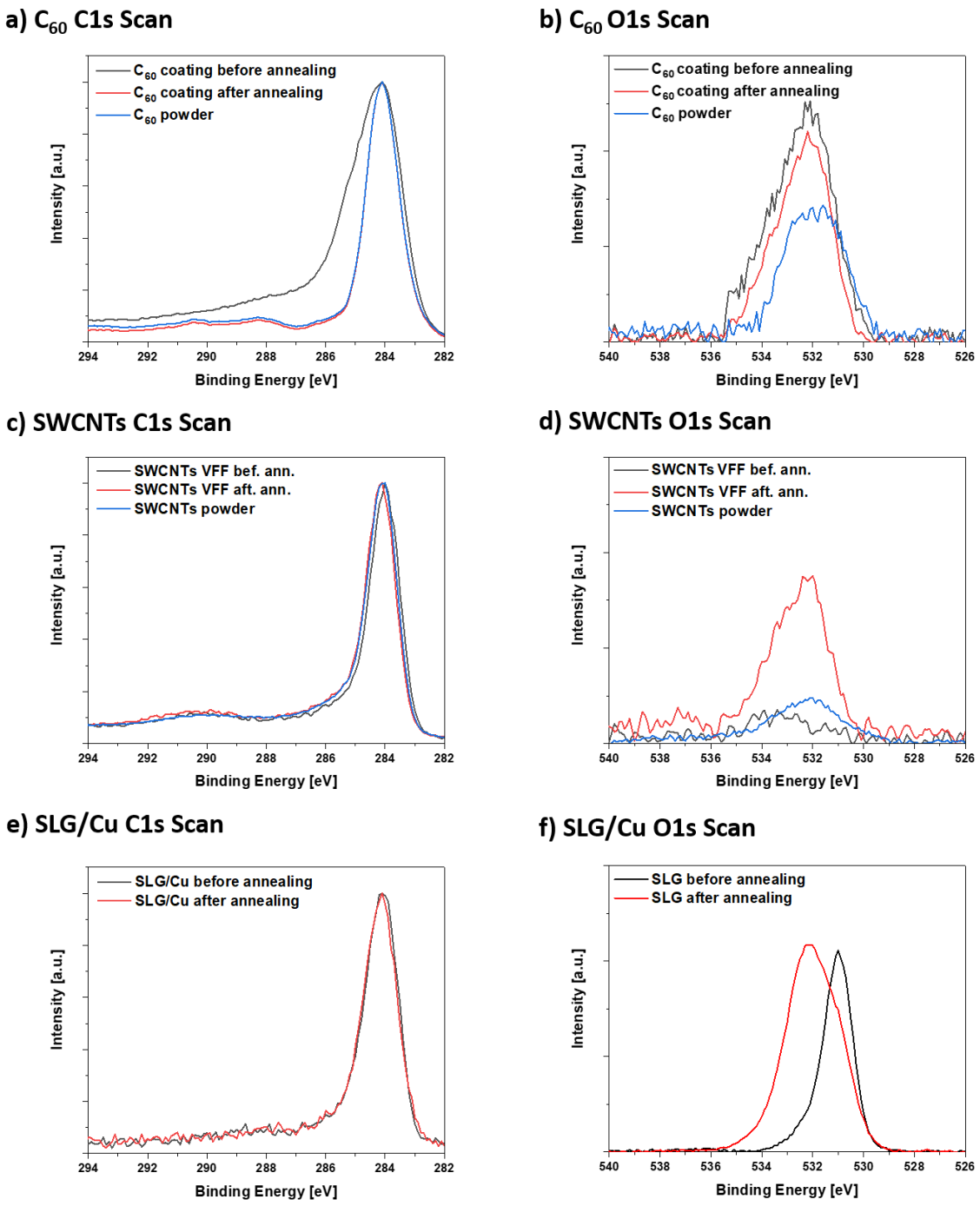

Figure 2. XPS spectra: C_{60} coatings before/after annealing and C_{60} powder used to manufacture coating – a) C1s scan and b) O1s scan, SWCNTs VFFs before/after annealing and SWCNTs powder used to create it – c) C1s scan and d) O1s scan, SLG/Cu before/after annealing – e) C1s scan and f) O1s scan.

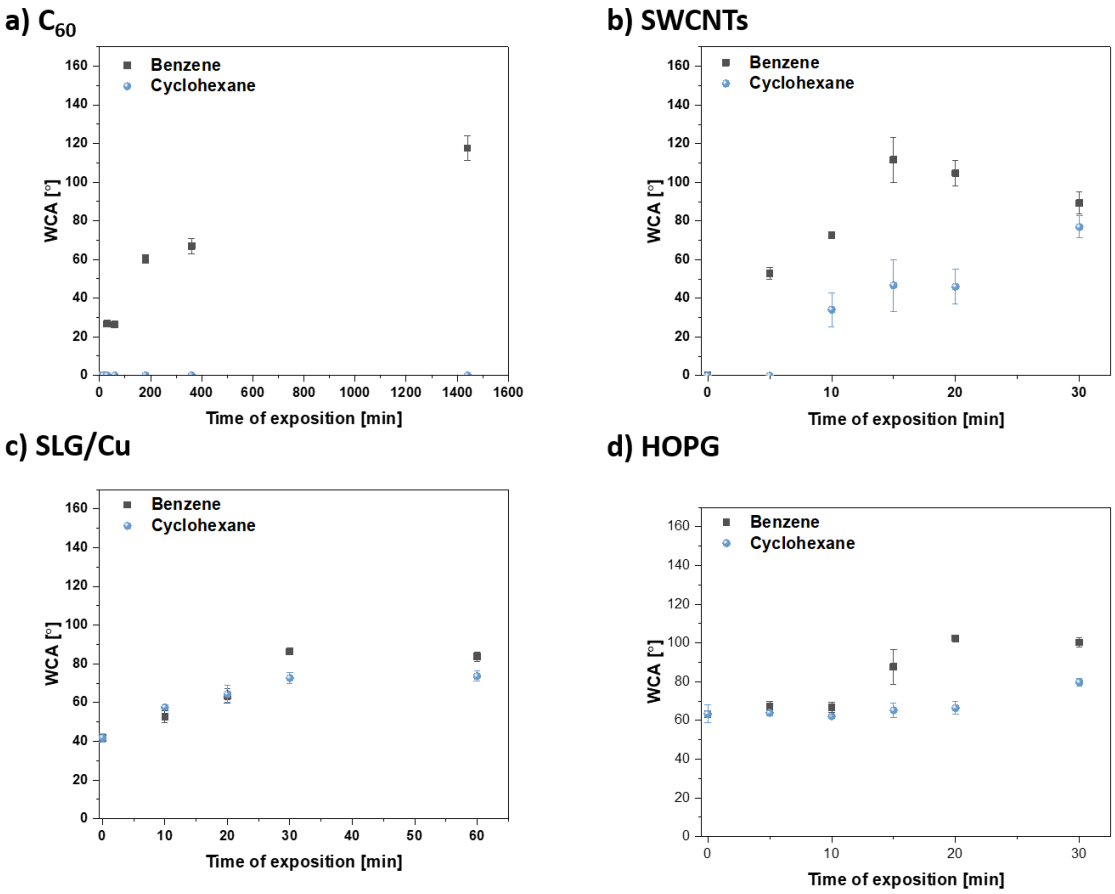

Figure 3. WCAs values of samples: a) C_{60}, b) SWCNTs, c) SLG/Cu, and d) HOPG, which were exposed to cyclohexane (sp^3) and benzene (sp^2) vapors (for the specified time), which have a similar vapor pressure.

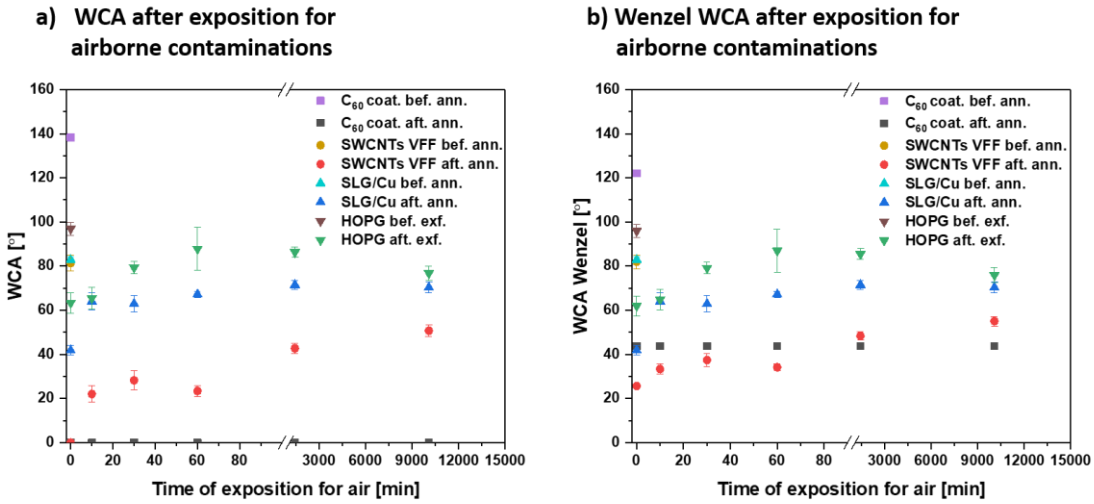

Figure 4. Measured evolution of WCA for carbon materials as a function of time of exposition to air a) and b) WCA computed by Wenzel model. C_{60} coat. bef. ann. – C_{60} coating before annealing exposed to atmospheric air for more than three months after manufactured coating, C_{60} coat. aft. ann. – C_{60} coating after annealing and then exposed to air in selected time periods, SWCNTs VFF bef. ann. – SWCNTs VFF before annealing exposed to atmospheric air for more than three months after manufactured VFF, SWCNTs VFF aft. ann. – SWCNTs VFF after annealing and then exposed to air in selected time periods, SLG/Cu bef. ann. – SLG/Cu before annealing exposed to atmospheric air for more than three months after synthesis, SLG/Cu aft. ann. – SLG/Cu after annealing and then exposed to air in selected time periods, HOPG bef. exf. – HOPG exposed to atmospheric air for more than three months after exfoliation, HOPG aft. exf. – HOPG after exfoliation and then exposed to air in selected time periods.

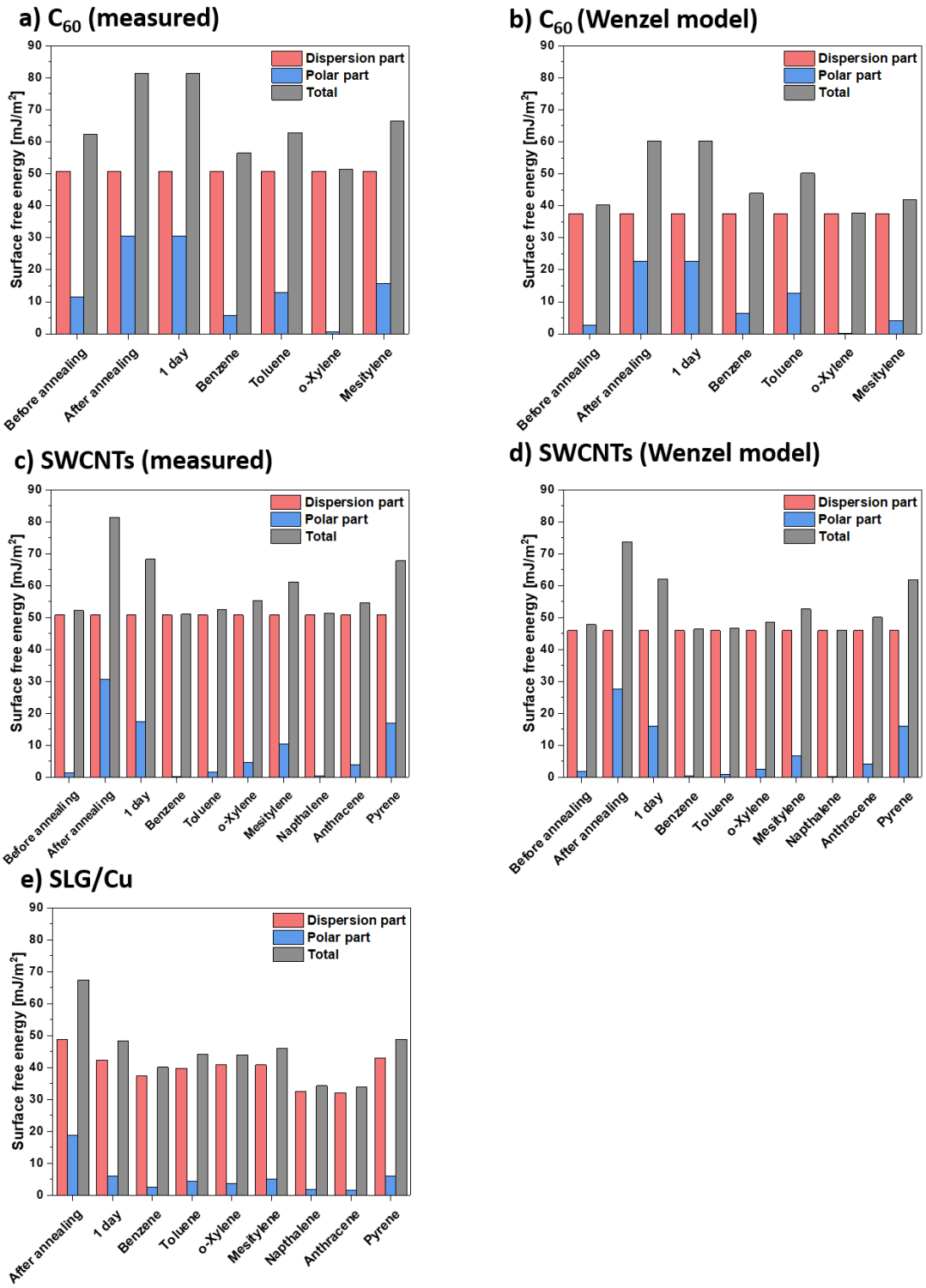

Figure 5. Surface free energy of prepared samples: a) C_{60} measured from experiments, b) C_{60} coatings computed using contact angle recalculated using the Wenzel model, c) SWCNTs VFFs measured from experiments, d) SWCNTs VFFs computed using contact angle recalculated using the Wenzel model and e) SLG/Cu foil measured from experiments.

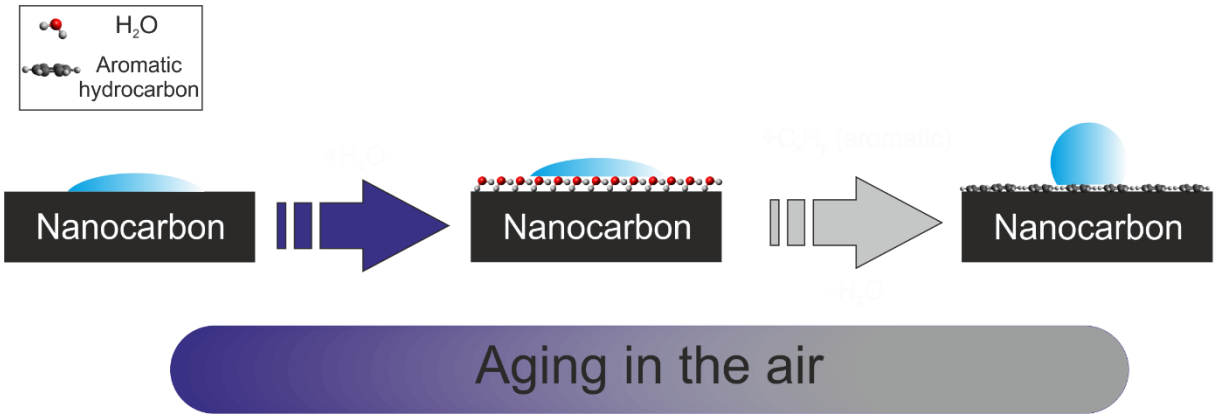

Figure 6. Mechanism of the phenomenon of hydrophobization of nanocarbon surface.

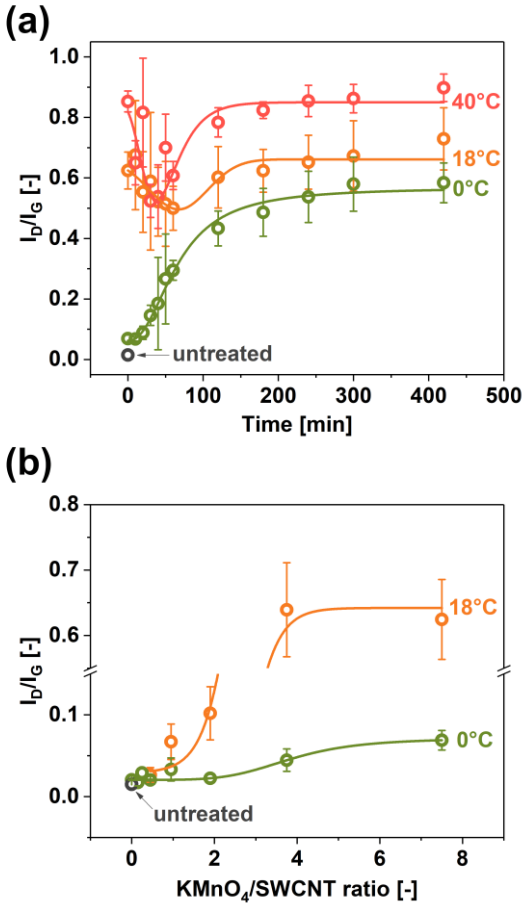

Figure 7. Results of investigation of the effect of SWCNT oxidation on the I_D/I_G ratio of the final product as a function of (a) time ($KMnO_4$/SWCNTs=7.5), and (b) $KMnO_4$/SWCNT ratio (t=0 min). Reproduced with permission from ref. [4] Copyright © 2022, Nature Publishing Group.

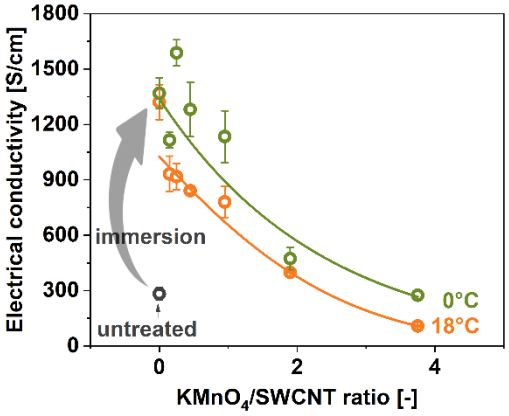

Figure 8. The impact of SWCNT oxidation on the electrical conductivity of the DFs made from oxidized SWCNTs as a function of the $KMnO_4$/SWCNT ratio (t=0 min). Reproduced with permission from ref. [4] Copyright © 2022, Nature Publishing Group.

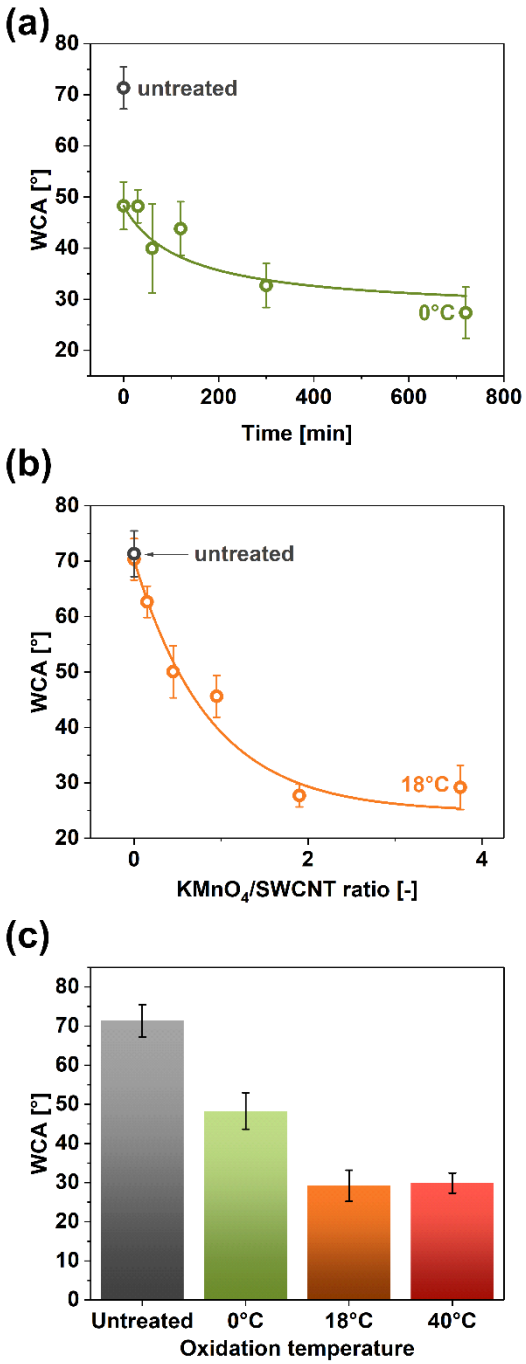

Figure 9. WCA as a function of (a) time (T=0 °C, $KMnO_4$/SWCNT=7.5), (b) $KMnO_4$/SWCNT ratio (T=18 °C, t=0 min), and (c) temperature ($KMnO_4$/SWCNT=7.5, t=0 min). Reproduced with permission from ref. [4] Copyright © 2022, Nature Publishing Group.

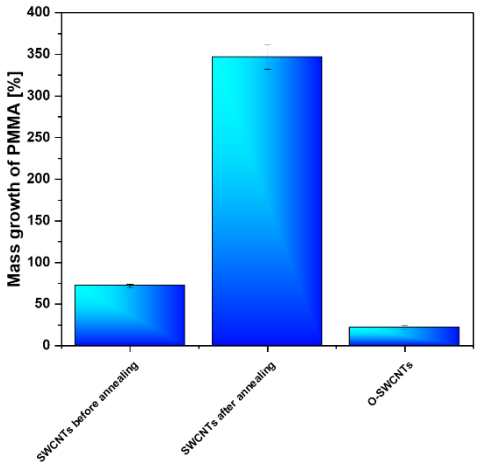

Figure 10. Mass growth of PMMA after dip-coating onto VFFs: SWCNTs before annealing – SWCNT VFF before annealing, SWCNTs after annealing – SWCNT VFF after annealing, O-SWCNTs – VFF from oxidized SWCNTs.

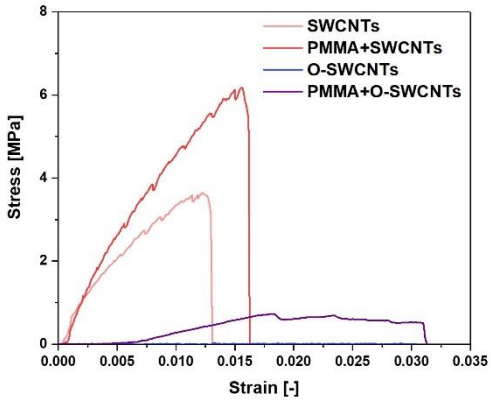

Figure 11. Mechanical tests of SWCNTs, PMMA+SWCNTs, O-SWCNTs and PMMA+O-SWCNTs.

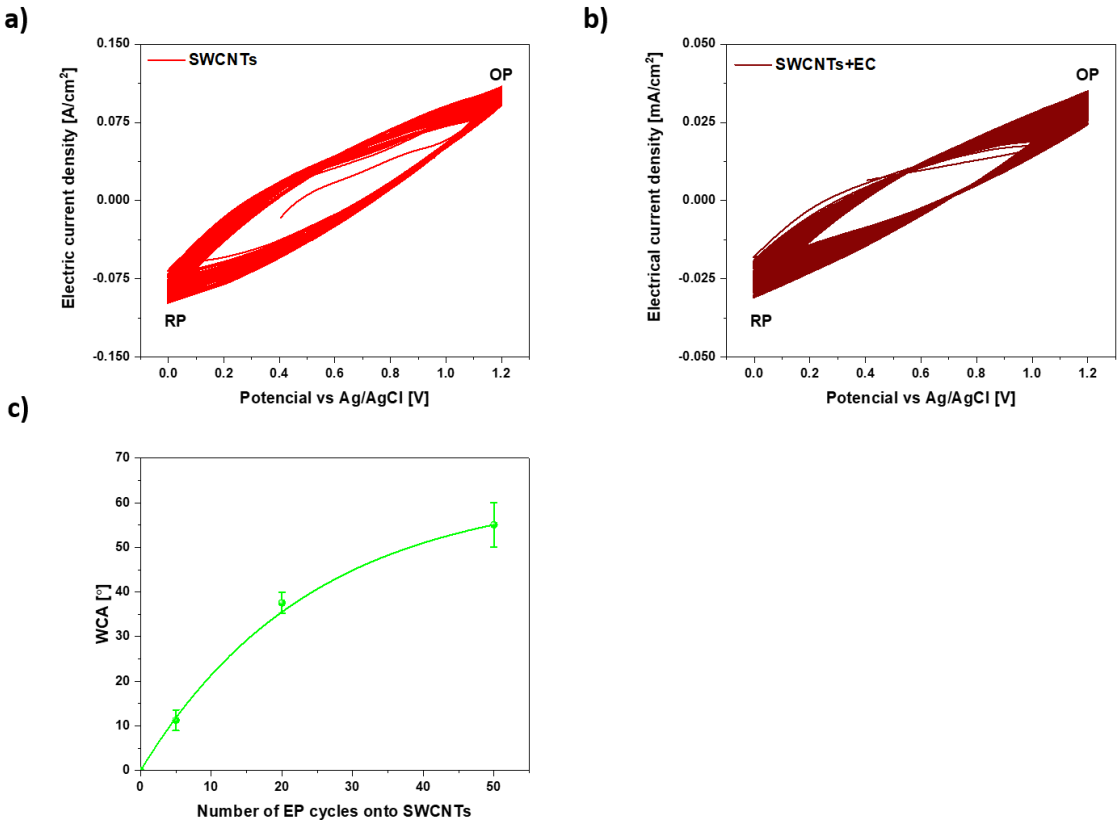

Figure 12. CV curves of aniline electropolymerization process onto SWCNTs DFEs using different potential ranges, where has been marked reduction peak (RP) and oxidation peak (OP) [(0.0 V) – (1.2 V)]: a) SWCNTs and b) SWCNTs+EC. c) Evolution of WCA depending on the number of EP cycles onto SWCNTs reproduced with permission from ref. [5] © 2023 Grzegorz Stando, Paweł Stando, Mika Sahlam, Mari Lundström, Haitao Liu Dawid Janas. Published by Elsevier B.V.

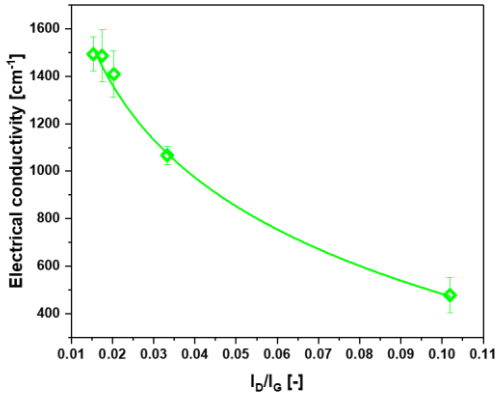

Figure 13. Raman spectroscopic analysis of the evolution of electrical conductivity as a function of I_D/I_G ratio of SWCNTs and O-SWCNTs used to create composites with PANI. Reproduced

with permission from ref. [5] © 2023 Grzegorz Stando, Paweł Stando, Mika Sahlam, Mari Lundström, Haitao Liu Dawid Janas. Published by Elsevier B.V.

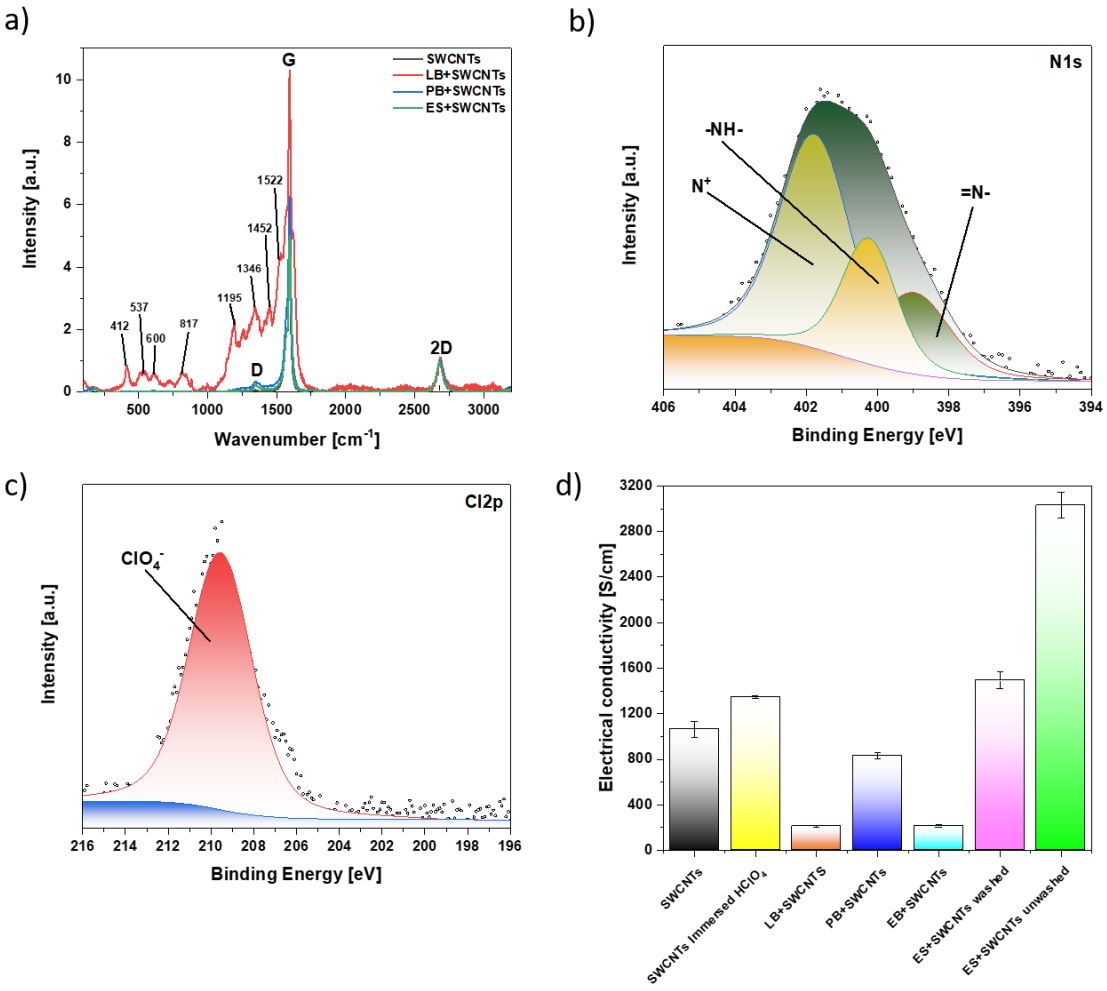

Figure 14. a) Raman spectra of PANI+SWCNTs composites normalized to 2D peak, b) XPS spectrum (N1s area) after 20 cycles of EP of ES+SWCNTs, c) XPS spectrum (Cl2p area) after 20 EP cycles of ES+SWCNTs, d) electrical conductivity of the synthesized composites. Reproduced with permission from ref. [5]© 2023 Grzegorz Stando, Paweł Stando, Mika Sahlam, Mari Lundström, Haitao Liu Dawid Janas. Published by Elsevier B.V.

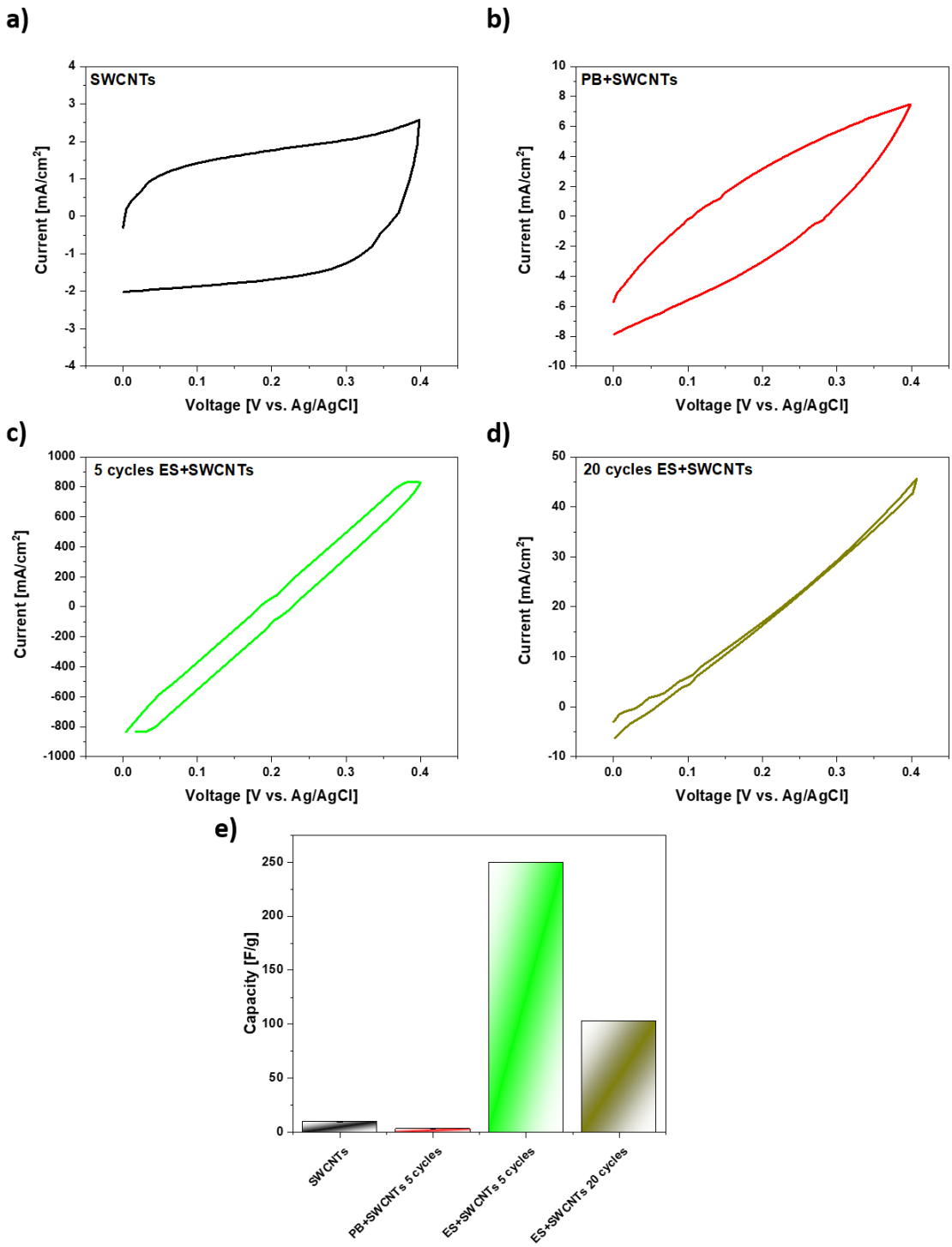

Figure 15. CV curves were employed for measuring: a) supercapacitor made of SWCNT DFEs; b) PB+SWCNTs EP for five cycles; c) ES+SWCNTs EP for five cycles; and d) ES+SWCNTs EP for twenty cycles, f) Capacities of manufactured supercapacitors. a), b), c), and d) were reproduced with permission from ref. [5]© 2023 Grzegorz Stando, Paweł Stando, Mika Sahlam, Mari Lundström, Haitao Liu Dawid Janas. Published by Elsevier B.V.

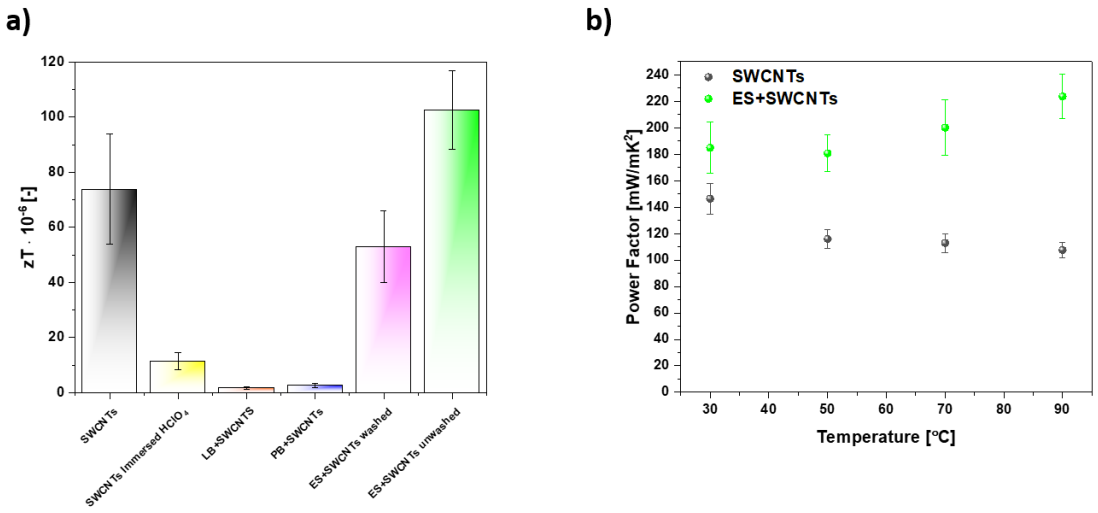

Figure 16. a) zT for nanomaterials produced at 30 ºC and b) temperature effects on the values of Power Factor.

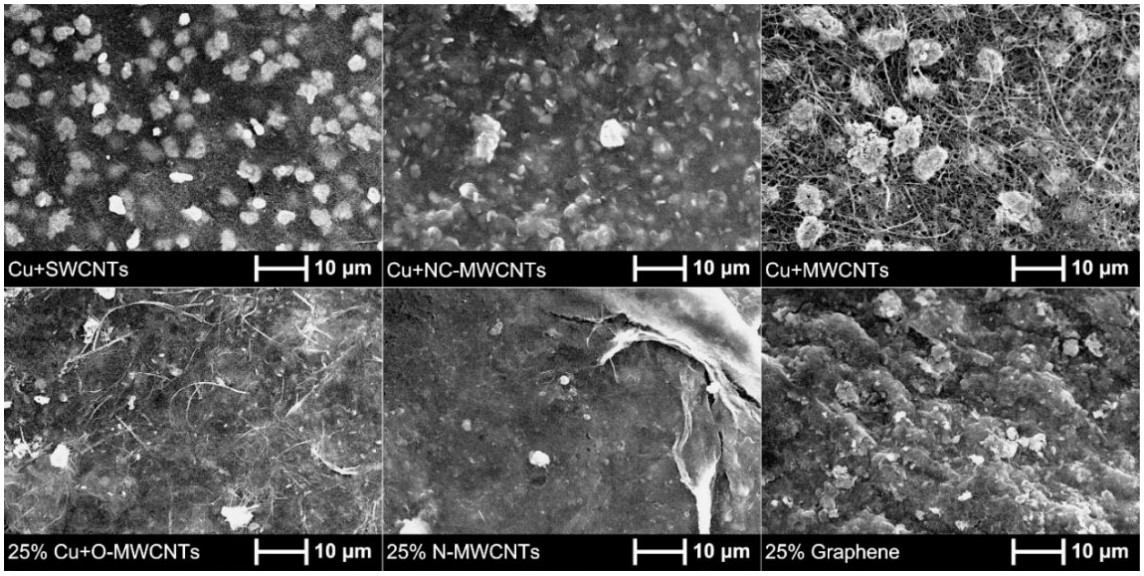

Figure 17. SEM micrographs of recovered copper deposit via electrodeposition on DFEs from nanocarbon materials. Reproduced with permission from ref. [6] © 2021 Grzegorz Stando, Pyry-Mikko Hannula, Bogumiła Kumanek, Mari Lundström, Dawid Janas. Published by Elsevier B.V.

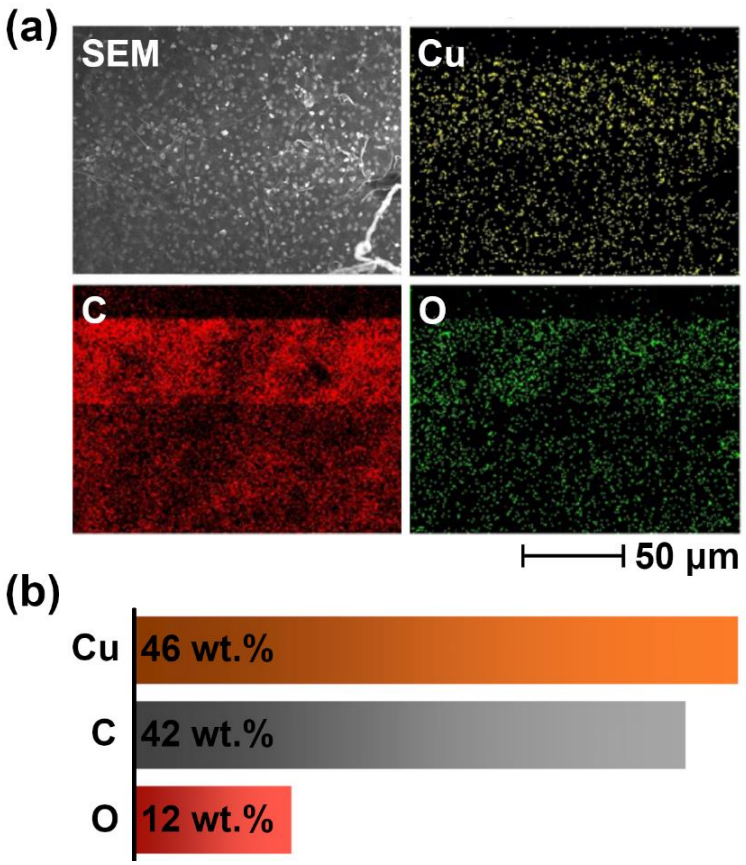

Figure 18. Cu-SWCNT composite (a) EDX mapping and (b) quantitative analysis. Reproduced with permission from ref. [6] © 2021 Grzegorz Stando, Pyry-Mikko Hannula, Bogumiła Kumanek, Mari Lundström, Dawid Janas. Published by Elsevier B.V.

Table 1. Composition of used wastewaters for recovery copper via electrodeposition Reproduced with permission from ref. [6] © 2021 Grzegorz Stando, Pyry-Mikko Hannula, Bogumiła Kumanek, Mari Lundström, Dawid Janas. Published by Elsevier B.V.

Solution	Mg [mg/L]	Al [mg/L]	Fe [mg/L]	Ni [ppm]	Cu [ppm]	Zn [ppm]	As [ppm]	Sb [ppm]	Pb [ppm]
Synthetic solution	-	-	-	-	40.0×10^6	-	-	-	-
Industrial process wastewater	6600	1400	12500	13	428	100	52	-	4.5

Main publication

1. Yang, F.*, **Stando, G.***, Thompson, A., Gundurao, D., Li, L., Liu, H. Effect of Environmental Contaminants on the Interfacial Properties of Two-Dimensional Materials. *Acc. Mater. Res.* **3** (10), 1022–1032 (2022). doi: 10.1021/accountsmr.2c00114
   * – authors contributed equally to this article.

   My participation was writing the original version of chapters "2. Effect of hydrocarbon contaminants on hexagonal two-dimensional materials and "3. Effect of other environmental contaminants on hexagonal two-dimensional materials", co-author of conclusions, Figure 1, and graphical abstract.

   My percentage in this publication is 35%

2. **Stando, G.,** Han, S., Kumanek, B., Łukowiec, D., Janas, D. Tuning wettability and electrical conductivity of single-walled carbon nanotubes by the modified Hummers method. Sci. Rep. 12, 4358 (2022). doi: 10.1038/s41598-022-08343-5 (IF=4.996; 140 pkt)

   My participation was conducting 80% of all experiments, data analysis, co-creating a research plan, and writing a draft of the manuscript.

   My percentage in this publication is 50%

3. **Stando, G.,** Hannula, P.M., Kumanek, B., Lundström, M., Janas, D. Copper recovery from industrial wastewater - Synergistic electrodeposition onto nanocarbon materials. Water Resour. Ind. 26, 100156 (2021). doi: 10.1016/j.wri.2021.100156 (IF= 4.206; 200 pkt)

   My participation was conducting all experiments and characterization, data analysis, participation in creating a research plan and writing a draft of the manuscript.

   My percentage in this publication is 50%

4. **Stando, G.**, Stando, P., Sahlman, M., Lundström, M., Liu, H., Janas, D. Synthesis of nanocomposites via electropolymerization of aniline onto hydrophilic films from nanocarbon and investigation of their properties, *Electrochim. Acta* **463**, 142842 (2023), https://doi.org/10.1016/j.electacta.2023.142842,

   My participation was co-creating a research plan, synthesis of half of the samples, characterization of samples by Raman, XPS and mechanical properties, creation and characterization by CV analysis supercapacitors, data analysis, writing an manuscript draft, contribution to revision of the manuscript after review.

   My percentage in this publication is 50%

References:

[1] D. Janas, G. Stando, Unexpectedly strong hydrophilic character of free-standing thin films from carbon nanotubes, Sci. Rep. 7 (2017). doi:10.1038/s41598-017-12443-y.

[2] G. Stando, D. Łukawski, F. Lisiecki, D. Janas, Intrinsic hydrophilic character of carbon nanotube networks, Appl. Surf. Sci. 463 (2019) 227–233. doi:10.1016/j.apsusc.2018.08.206.

[3] F. Yang, G. Stando, A. Thompson, D. Gundurao, L. Li, H. Liu, Effect of Environmental Contaminants on the Interfacial Properties of Two-Dimensional Materials, Accounts Mater. Res. 3 (2022) 1022–1032. doi:10.1021/accountsmr.2c00114.

[4] G. Stando, S. Han, B. Kumanek, D. Łukowiec, D. Janas, Tuning wettability and electrical conductivity of single-walled carbon nanotubes by the modified Hummers method, Sci. Rep. 12 (2022) 1–13. doi:10.1038/s41598-022-08343-5.

[5] G. Stando, P. Stando, M. Sahlman, M. Lundstrom, H. Liu, D. Janas, Synthesis of nanocomposites via electropolymerization of aniline onto hydrophilic films from nanocarbon and investigation of their properties, Electrochim. Acta. 463 (2023) 142842. doi:10.1016/j.electacta.2023.142842.

[6] G. Stando, P.-M. Hannula, B. Kumanek, M. Lundström, D. Janas, Copper recovery from industrial wastewater - Synergistic electrodeposition onto nanocarbon materials, Water Resour. Ind. 26 (2021) 100156. doi:10.1016/J.WRI.2021.100156.

[7] H.W. Kroto, J.R. Heath, S.C. O'Brien, R.F. Curl, R.E. Smalley, C60: Buckminsterfullerene, Nature. 318 (1985) 162–163. doi:10.1038/318162a0.

[8] J.N. Coleman, U. Khan, W.J. Blau, Y.K. Gun'ko, Small but strong: A review of the mechanical properties of carbon nanotube-polymer composites, Carbon N. Y. 44 (2006) 1624–1652. doi:10.1016/j.carbon.2006.02.038.

[9] F. Mansoori Mosleh, Y. Mortazavi, N. Hosseinpour, A.A. Khodadadi, Asphaltene Adsorption onto Carbonaceous Nanostructures, Energy and Fuels. 34 (2020) 211–224. doi:10.1021/acs.energyfuels.9b03466.

[10] S. Pei, J. Zhao, J. Du, W. Ren, H.M. Cheng, Direct reduction of graphene oxide films into highly conductive and flexible graphene films by hydrohalic acids, Carbon N. Y. 48 (2010) 4466–4474. doi:10.1016/j.carbon.2010.08.006.

[11] C. Soldano, A. Mahmood, E. Dujardin, Production, properties and potential of graphene, Carbon N. Y. 48 (2010) 2127–2150. doi:10.1016/J.CARBON.2010.01.058.

[12] B. Kumanek, D. Janas, Thermal conductivity of carbon nanotube networks: a review, J. Mater. Sci. 54 (2019) 7397–7427. doi:10.1007/s10853-019-03368-0.

[13] F. Cesano, M.J. Uddin, K. Lozano, M. Zanetti, D. Scarano, All-Carbon Conductors for Electronic and Electrical Wiring Applications, Front. Mater. 7 (2020). doi:10.3389/fmats.2020.00219.

[14] N.M. Nurazzi, M.R.M. Asyraf, A. Khalina, N. Abdullah, C.L. Lee, H.A. Aisyah, M. Nor, F. Norrrahim, R.A. Ilyas, M.M. Harussani, M.R. Ishak, Nanotube-Reinforced Polymer Composite : An Overview, Polymers (Basel). 13 (2021) 1047.

[15] M. Bhattacharya, Polymer nanocomposites-A comparison between carbon nanotubes, graphene, and clay as nanofillers, Materials (Basel). 9 (2016) 1–35. doi:10.3390/ma9040262.

[16] F.G. Granados-Martínez, J.J. Contreras-Navarrete, D.L. García-Ruiz, C.J. Gutiérrez-García, A. Durán-Navarro, E.E. Gama-Ortega, N. Flores-Ramírez, E. Huipe-Nava, L. García-González, M. de L. Mondragón-Sánchez, L. Domratcheva-Lvova, Carbon Nanotubes Synthesis from Four

Different Organic Precursors by CVD, MRS Proc. 1817 (2016) imrc2015abs070-abs308. doi:10.1557/opl.2016.53.

[17] C. Bartholome, P. Miaudet, A. Derré, M. Maugey, O. Roubeau, C. Zakri, P. Poulin, Influence of surface functionalization on the thermal and electrical properties of nanotube-PVA composites, Compos. Sci. Technol. 68 (2008) 2568–2573. doi:10.1016/j.compscitech.2008.05.021.

[18] I. Gerber, M. Oubenali, R. Bacsa, J. Durand, A. Gonçalves, M.F.R. Pereira, F. Jolibois, L. Perrin, R. Poteau, P. Serp, Theoretical and Experimental Studies on the Carbon-Nanotube Surface Oxidation by Nitric Acid: Interplay between Functionalization and Vacancy Enlargement, Chem. - A Eur. J. 17 (2011) 11467–11477. doi:10.1002/chem.201101438.

[19] V. Datsyuk, M. Kalyva, K. Papagelis, J. Parthenios, D. Tasis, A. Siokou, I. Kallitsis, C. Galiotis, Chemical oxidation of multiwalled carbon nanotubes, Carbon N. Y. 46 (2008) 833–840. doi:10.1016/j.carbon.2008.02.012.

[20] N.F. Andrade, D.S.T. Martinez, A.J. Paula, J. V. Silveira, O.L. Alves, A.G. Souza Filho, Temperature effects on the nitric acid oxidation of industrial grade multiwalled carbon nanotubes, J. Nanoparticle Res. 15 (2013) 1–11. doi:10.1007/s11051-013-1761-8.

[21] Y.C. Chiang, W.H. Lin, Y.C. Chang, The influence of treatment duration on multi-walled carbon nanotubes functionalized by H2SO4/HNO3 oxidation, Appl. Surf. Sci. 257 (2011) 2401–2410. doi:10.1016/j.apsusc.2010.09.110.

[22] I.D. Rosca, F. Watari, M. Uo, T. Akasaka, Oxidation of multiwalled carbon nanotubes by nitric acid, Carbon N. Y. 43 (2005) 3124–3131. doi:10.1016/j.carbon.2005.06.019.

[23] G. Otero, G. Biddau, C. Sánchez-Sánchez, R. Caillard, M.F. López, C. Rogero, F.J. Palomares, N. Cabello, M.A. Basanta, J. Ortega, J. Méndez, A.M. Echavarren, R. Pérez, B. Gómez-Lor, J.A. Martín-Gago, Fullerenes from aromatic precursors by surface-catalysed cyclodehydrogenation, Nature. 454 (2008) 865–868. doi:10.1038/nature07193.